RESEARCH ARTICLE

Check for updates

Defect-engineering a metal−organic framework for CO$_2$ fixation in the synthesis of bioactive oxazolidinones†

Aasif Helal, [iD] *[a] Kyle E. Cordova, [iD] [b] Md. Eyasin Arafat,[a] Muhammad Usman [iD] [a] and Zain H. Yamani [iD] [a]

A novel series of UiO-66 structures with linker-induced defects was synthesized and fully characterized. By using a linker functionalized with a free, dangling alkylamine that replaces the ordinary carboxylate coordinating group, up to 40% of the linkers incorporated within the UiO-66 framework were defect sites. The resulting UiO-66 with linker-induced defects was then demonstrated to be a highly active heterogeneous catalyst. When applied to three-component, solvent-free cycloadditions of epoxides with aromatic amines and CO$_2$ at ambient pressure, a diverse range of bioactive oxazolidinone compounds were isolated in significantly high yields (>90%) with quantitative conversions and regioselectivity. Finally, the catalyst was proven recyclable over 5 consecutive reactions without loss of performance.

Introduction

It is becoming increasingly clear that the economics behind reducing CO$_2$ emissions from the atmosphere is not favorable enough to implement solutions that quickly solve the global climate change problem.[1] As a result, significant efforts have turned toward advancing the chemical utilization of CO$_2$ as a C1 building block for producing fine chemicals with added economic value.[2] Although this approach is in itself quite challenging, given that CO$_2$ is a thermodynamically stable molecule, there are important classes of compounds that have the potential to use CO$_2$ as a building block in their production.[3]

One such class is oxazolidinones; five-membered heterocyclic compounds that have found application as antibiotics (*e.g.* tedizolid, posizolid, linezolid, and radezolid, among others) due to their activity against a large spectrum of Gram-positive bacteria.[4] Conventional synthesis of oxazolidinones

dictates the use of either poisonous phosgenes or toxic isocyanates as the source of the oxazolidinone's carbonyl carbon.[5] Due to the hazardous nature of these starting materials, CO$_2$ and/or cyclic organic carbonates (derived from CO$_2$ cycloaddition with epoxides) have been explored as alternative sources for the carbonyl carbon when pursuing other more benign synthetic routes such as, the dehydration of vicinal amino alcohols with CO$_2$, the cycloaddition of aziridines to CO$_2$, aminolysis of cyclic carbonates, and the cyclization of unsaturated amines with CO$_2$.[6] However, there remain significant drawbacks to these routes as a result of the requisite high pressures of CO$_2$ needed, expensive and complex synthesis of metal catalysts employed, poor recyclability due to the homogeneous nature of the catalysts, and limitations of heterogenous systems with respect to substrate scope.[2,6]

Metal–organic frameworks (MOFs) are an extensive class of porous, crystalline materials whose backbone architecture can be precisely controlled on the atomic level for gas capture and subsequent catalytic conversions.[7] Premediated incorporation of defects within the backbone of MOF structures disrupts the regular, periodic arrangements of atoms throughout its crystal lattice and allows for the realization of enhanced catalytic properties due to more easily accessible active sites.[8] Engineered or inherently-found defects have contributed to enhanced catalytic activities of MOFs when applied in Paal–Knorr reactions, various Brønsted- and Lewis-acid catalyzed reactions, esterification, cyanosilylation, methanolysis, Knoevenagel condensation, oxidation of alkenes, and Michael additions, among others.[9] Such defect sites have also been used to introduce cat-

[a]*Center of Research Excellence in Nanotechnology (CENT), King Fahd University of Petroleum and Minerals (KFUPM), Dhahran 31261, Saudi Arabia.*
E-mail: aasifh@kfupm.edu.sa
[b]*Materials Discovery Research Unit, Reticular Foundry, Royal Scientific Society, Amman 11941, Jordan*

†Electronic supplementary information (ESI) available: Full synthesis and characterization details for all MOFs presented herein including, but not limited to, powder X-ray diffraction, digestion ^{1}H NMR, FT-IR, thermal gravimetric analysis curves, and gas adsorption isotherms. Full characterization details (^{1}H and ^{13}C NMR) of all of the products obtained from the catalysis experiments; finally, structural and mechanistic studies for the catalytic processes. See DOI: 10.1039/d0qi00496k

alytically active species or, at times, to increase the vacancies of the linker throughout the structure.[10] Regardless of these successes and/or approaches, there have been very few MOF catalysts, defect-engineered or not, employed in the synthesis of important classes of bioactive compounds like oxazolidinones using CO_2 as a building block.[11]

The present work describes a general method for introducing linker-induced defects within a well-known zirconium-based MOF, UiO-66,[12,13] that creates two structural advantages (Fig. 1): (i) formation of vacant coordination sites within the MOFs' inorganic secondary building unit (SBU), thereby promoting Zr(IV) as a functional Lewis acid catalytic site;[14] and (ii) judicious incorporation of a linker that is functionalized with an alkylamine thereby enhancing CO_2 uptake and, later, enabling the linker to serve as a co-catalyst to realize the end oxazolidinone products. Accordingly, through this method, we herein report a highly active and efficient heterogeneous catalyst for three-component cycloadditions of epoxides with aromatic amines and CO_2 that produce a diverse range of oxazolidinone compounds in significantly high yields with quantitative conversions and selectivity.
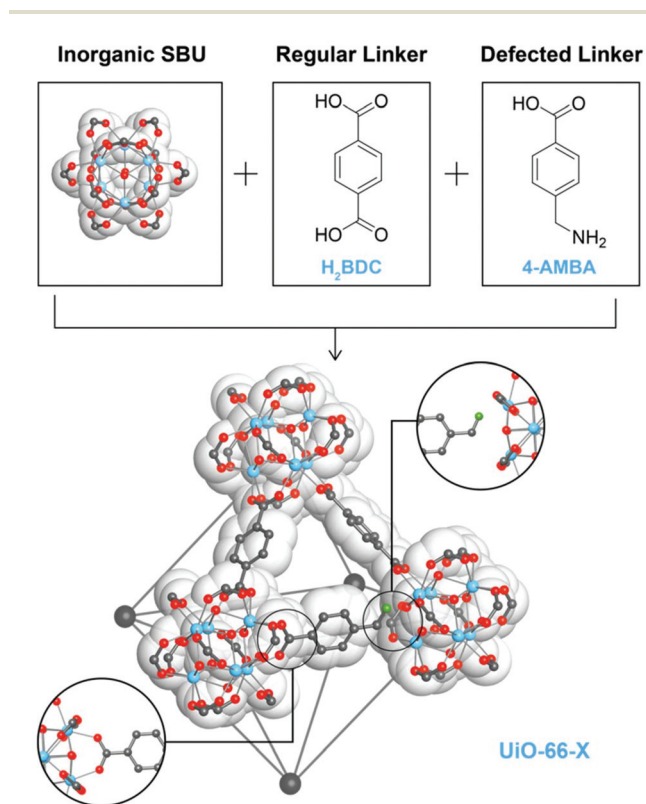

Fig. 1 General synthetic strategy for engineering linker-induced defects within the zirconium-based metal–organic framework, UiO-66. As a result of a missing carboxylate coordinating group, there exists a free, dangling alkylamine. Atom colors: Zr, blue; C, grey; N, green; and O, red. All H atoms are removed for clarity. H_2BDC = 1,4-benzene dicarboxylic acid; 4-AMBA = 4-(aminomethyl)benzoic acid; UiO-66-*X*, where *X* is the output mol% ratio of 4-AMBA (*X* = 10, 20, 30, and 40, respectively).

Experimental

Materials and characterization

Chemicals and supplies. 1,4-Benzene dicarboxylic acid (H_2BDC; 98% purity), zirconium tetrachloride ($ZrCl_4$; 99.99% purity), 4-(aminomethyl)benzoic acid (4-AMBA; 97% purity), methanol (99.9% purity), *N*,*N*′-dimethylformamide (DMF; 99.8% purity), dichloromethane (99.8% extra dry grade), aniline (99%) with all the other aromatic amines, and propylene oxide (99%) with all the other epoxides were purchased from Sigma Aldrich. Nuclear magnetic resonance spectroscopy (NMR) solvents: chloroform-*d* (CDCl₃; 99.9% purity) and dimethyl sulfoxide-*d₆* (DMSO-*d₆*; 99.9% purity) were purchased from Cambridge Isotope. All chemicals were used without further purification. Water used in this work was doubly distilled and filtered through a Millipore membrane.

Characterization. ^{1}H and ^{13}C NMR spectra were recorded on a Bruker AM-400 spectrometer using TMS as the internal standard. Powder X-ray diffraction (PXRD) patterns of the samples were recorded using a Rigaku MiniFlex diffractometer, which was equipped with Cu Kα radiation. The data were acquired over the 2θ range of 5 and 40°. The Fourier-transform infrared spectra (FT-IR) spectra were obtained using a Nicolet 6700 Thermo Scientific instrument in the range of 400–4000 cm⁻¹, using KBr pellets. Thermal gravimetric analysis (TGA) was conducted using a TA Instruments Q500 with the sample held in a platinum pan under airflow. The Brunauer–Emmett–Teller (BET) surface area of UiO-66 and its analogues were calculated by measuring a N_2 isotherm at 77 K on a Micromeritics ASAP 2020 instrument. A liquid nitrogen bath was used for the measurements at 77 K. CO_2 sorption isotherms were measured on an Autosorb iQ2 volumetric gas adsorption analyzer. The measurement temperatures at 273 and 298 K were controlled with a water circulator.

Synthesis of UiO-66 and its analogues with linker-induced defects. For full details of the synthesis of UiO-66 and its analogues with linker-induced defects, please refer to the ESI, sections S1 and S2.†

General synthesis of oxazolidinones from aromatic amines, epoxides, and CO_2. In a typical reaction, UiO-66 catalyst (70 mg), epoxide (6.0 mmol), and aromatic amine (2.0 mmol) were introduced into a 10 mL Schlenk flask. The flask was equipped with a balloon of CO_2, and the reaction mixture was stirred on a magnetic stirrer at 85 °C for 12 h. Upon completion of the reaction, the mixture was cooled to room temperature. The catalyst was separated by centrifugation with ethyl acetate three times. The combined ethyl acetate layer was concentrated, and the product was isolated by column chromatography (ethyl acetate/hexane). The product was characterized by ^{1}H and ^{13}C NMR spectra and the identities of the oxazolidinones were confirmed by comparison with literature data.

Results & discussion

Crystals of UiO-66 were prepared by adding $ZrCl_4$ to a DMF and acetic acid solution mixture containing dissolved 1,4-benzene dicarboxylic acid (H_2BDC; see ESI, section S1†).[12] In

order to produce UiO-66 analogues with linker-induced defects, 4-(aminomethyl)benzoic acid (4-AMBA) was added in four different mol% quantities (16, 27, 37, and 45 mol%, respectively) along with the normal H_2BDC linker under conditions similar to those previously used in the synthesis of the parent UiO-66 (Fig. 1 and ESI, Table S1†).[12,15] Powder X-ray diffraction (PXRD) analysis of the obtained MOFs demonstrated high crystallinity with diffraction patterns in satisfactory agreement with the diffraction pattern generated from the single crystal structure of UiO-66 (Fig. 2 and ESI, Fig. S2†). This indicates that the UiO-66 structure remains intact up to the point of introducing 45 mol% of the defect-inducing 4-AMBA. Beyond this, the material was found to be amorphous providing sufficient evidence that the structure could not sustain the number of defects generated. Prior to further analysis, all of the MOFs were washed, solvent-exchanged, and activated to ensure that any starting materials or by-products were removed.

To assess whether both linkers were incorporated within each structure and, if so, to quantify the degree of incorporation, digestion ^1H NMR was carried out by dissolving an activated sample of each MOF in a solution of NaOD/DMSO-d_6. The digestion NMR spectrum for each sample displayed the presence of both linkers and the relative ratios were then calculated by integration of appropriate peaks (ESI, Fig. S3–S7 and Table S2†). Although the input/output ratios of the linkers were found to be different, they were controllable, as expected, to a certain degree.[16] As a result, the UiO-66 analogues with linker-induced defects were named UiO-66-X with X representing the output mol% ratio of 4-AMBA as determined by ^1H NMR digestion (i.e. X = 10, 20, 30, and 40, respectively). Fourier-transform infrared spectroscopy measurements provided further support for incorporation of 4-AMBA. Accordingly, the spectra for UiO-66-10, -20, -30, and -40 each exhibit a new absorption band centered at ~1670 cm^{-1} and attributed to a N–H bending frequency, which increased in intensity as a function of increased incorporation of 4-AMBA (ESI, Fig. S8†). This band is not present in the spectrum of the parent UiO-66. Aside from this, the absorption bands found in the rest of the spectra correspond well to each other (e.g. $\nu_{C=O}$ = ~1390 cm^{-1} and ν_{O-H} = 3320–3430 cm^{-1}). Finally, chemical formulation for each MOF was determined by elemental analysis (ESI, section S1†).

The architectural robustness of the UiO-66 analogues with linker-induced defects were studied through a combination of thermal gravimetric analysis and N_2 adsorption isotherms at 77 K. Surprisingly, it was found that there was no loss in thermal stability in any of the UiO-66 structures as evidenced by a thermal stability reaching 500 °C for UiO-66-40 (ESI, Fig. S9†). This is likely due to the nature of the strong coordinate-covalent bonds formed between the hard acidic Zr(IV) and the hard basic carboxylate coordinating groups. N_2 isotherms at 77 K exhibit a consistent decrease in surface area across the series starting from 1100 m^2 g^{-1} for the parent UiO-66 to 600 m^2 g^{-1} for UiO-66-40 (ESI, Fig. S10†). The trend observed for the decreasing BET as a function of increasing defects is due to the increasing presence of dangling alkylamine groups within the pores of the MOF. Pore size distributions showed the opposite effect, as expected, by which the pores increased from 1.1 to 1.5 nm for UiO-66 to UiO-66-40, respectively (ESI, Fig. S11†).

Given the structures of the UiO-66 analogues with linker-induced defects, it can be reasonably concluded that there exist two possible active sites for exploitation in catalysis: (i) Lewis acidic sites originating from Zr(IV) in the SBUs; and (ii) basic sites originating from a free, dangling alkylamine (–CH_2NH_2) in 4-AMBA. The dangling alkylamine can act as a CO_2 activator by forming carbamate while, in tandem, the oxophilic Zr(IV) active sites can activate other substrate molecules for initiating further reactivity.[7] Following this line of thinking, we sought to first assess the series' adsorption/desorption of CO_2 at 273 and 298 K (ESI, Fig. S12–14†). The adsorption capacities at 1 bar varied, but, more importantly, a sharp uptake at low pressure, and a slight hysteresis was observed upon desorption for UiO-66-40 when it was not observed for UiO-66. Indeed, this provides indication that a stronger adsorption mechanism is occurring; an indication that was proven true upon calculation of the isosteric enthalpy of adsorption (Q_{ST}). The Q_{ST} for UiO-66-40 was high at 86 kJ mol^{-1}, which signifies that chemisorption is taking place between the alkylamine and CO_2.[17]

In order to highlight the catalyst potential of this series of MOFs, we chose a three-component reaction (1,2-epoxyhexane, aniline, and CO_2) as a model. This allowed for the optimization of conditions, including optimizing the number of linker-induced defects needed in the MOF catalyst, and maximization of conversion to the model oxazolidinone. As shown in Table 1, the parent UiO-66, without linker-induced defects, does not lead to any product formation in the presence of CO_2 (1 atm) and heating at 85 °C for 12 h. Similarly, there was no
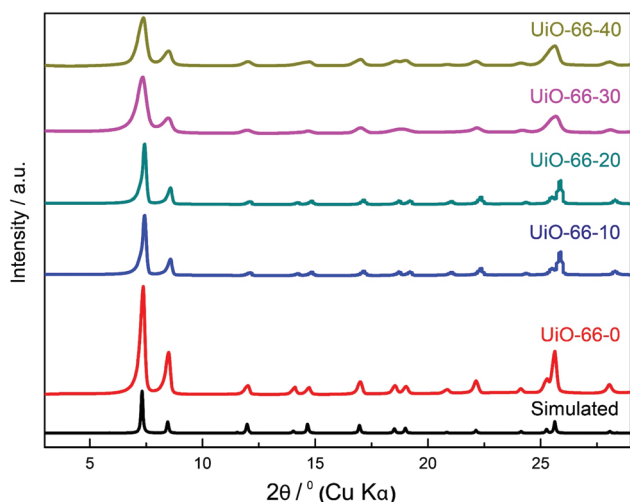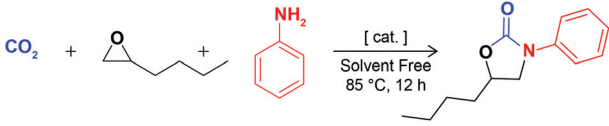

Fig. 2 Powder X-ray diffraction patterns for UiO-66 and the UiO-66 analogues with linker-induced defects. These experimental diffraction patterns are presented in comparison to the diffraction pattern simulated from the crystal structure of UiO-66.

Research Article

Table 1 Comparative study of catalysts for the three-component cycloaddition reaction of CO_2 with aniline and 1,2-epoxyhexane[a]

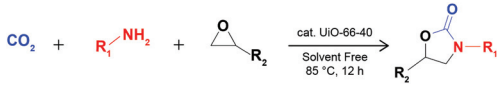| Entry	Catalyst	Yield[b] (%)
1	UiO-66	N.R.
2	UiO-66-10	N.R.
3	UiO-66-20	N.R.
4	UiO-66-30	42
5	UiO-66-40	87

[a] Reaction conditions: 1,2-epoxyhexane (6.0 mmol), aniline (2.0 mmol), CO_2 (1 bar), catalyst (70 mg), solvent-free, 12 h, 85 °C. [b] Isolated yield calculated with respect to aniline as determined by ^{1}H NMR spectroscopy. N.R., no reaction.

product formation when using UiO-66-10 and -20 as the catalyst under the prescribed conditions. However, as the incorporated linker-induced defects were increased from 10 and 20 mol% to 30 and 40 mol%, the conversion also increased reaching a maximum yield of 87% with UiO-66-40. No starting material remained present upon completion of the reaction, thereby affording a quantitative conversion.

To investigate the versatility of this catalyst with respect to amine-based substrate scope, reactions with various *para*-substituted aromatic amines were conducted using the optimized conditions. As demonstrated in Table 2, aromatic amines with electron-withdrawing groups, such as –NO_2, produced higher yields (94%) when compared with aromatic amines containing electron-donating groups (–CH_3 yield = 83% and –OCH_3 yield = 80%). Again, quantitative conversion was achieved for all such reactions. Additionally, we investigated the catalytic activity towards a sterically hindered amine that is attached to the nitrogen-rich, heteroaromatic adenine. This substrate resulted in the production of the corresponding oxazolidinone in 70% yield (Table 2, entry 7). The relatively lower yield was attributed to steric (*i.e.* bulkiness of heteroaromatic amine) and electronic (*i.e.* electron-donating nature of the adenine ring) effects. Interestingly, when using a primary amine-based substrate, such as benzylamine, the reaction failed to proceed toward the respective oxazolidinone product.

The diversity in substrate scope was not only limited to aromatic amines. Different substituted epoxides were also chosen to react with aniline and CO_2 using the optimized conditions (Table 2, entries 9–14). From these reactions, a general trend was observed in that all monosubstituted aliphatic and aromatic epoxides produce high yields of the corresponding oxazolidinone product (78–90%) with quantitative conversion. The reaction produced similarly high yields when bulky, disubstituted epoxides (*i.e.* cyclohexane oxide) were used as substrates (Table 2, entry 14). It is important to note in each reaction that UiO-66-40 was employed as a catalyst, the only product isolated was the 5-substituted oxazolidinone. Given

Table 2 Reaction scope for the three-component cycloaddition of CO_2 with aromatic amines and substituted epoxides in the presence of UiO-66-40 as a heterogeneous catalyst[a]

Entry	Aromatic amine	Epoxide	Product	Yield[b] (%)
1				87
2				94
3				83
4				80
5				91
6				81
7				70
8			—	—
9				90
10				89
11				87
12				78
13				85
14				73

[a] Reaction conditions: epoxide (6.0 mmol), aromatic amine (2.0 mmol), CO_2 (1 bar), UiO-66-40 catalyst (70 mg), solvent-free, 12 h, 85 °C. [b] Isolated yield calculated with respect to aromatic amine as determined by ^{1}H NMR spectroscopy.

that there was no evidence of any 4-substituted oxazolidinone products being formed, it can be concluded that the catalyst is 100% regioselective. This is likely due to steric hindrance between the aromatic amines, epoxide side chains, and the internal pore environment of the UiO-66-40 catalyst.

From a mechanistic standpoint, we believe that both active sites are critical for the reaction's success (Fig. 3). The SBU of UiO-66 has six Lewis acidic Zr(IV) active sites and, from digestion ^{1}H NMR data, 0.64 4-AMBA linkers per BDC^{2-} linker are also present (ESI, Fig. S7 and Table S2†).[12,18] Accordingly, the free alkylamines act as activators of CO_2 by forming carbamates upon adsorption. At the same time, the epoxide substrates coordinate to the Zr(IV) sites to form intermediate **1**. This adduct undergoes a nucleophilic attack by the carbamate that results in the ring opening of the epoxide substrate to
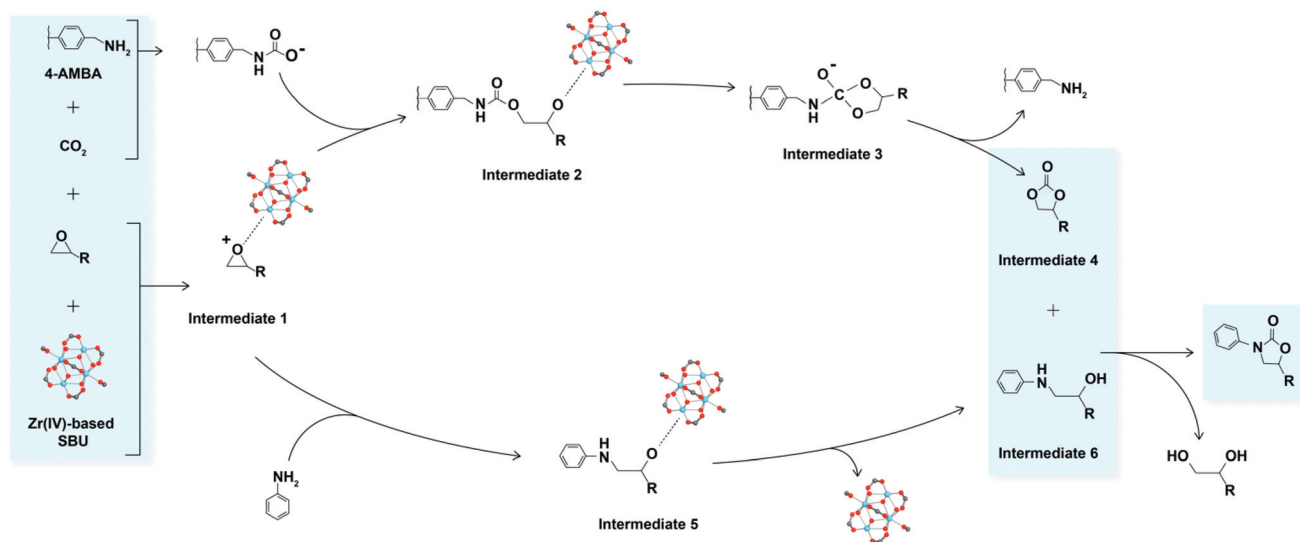
Fig. 3 Proposed mechanism for the synthesis of oxazolidinones from a three-component reaction catalyzed by UiO-66-40. Atom colors: Zr, blue; C, grey; and O, red. All H atoms omitted for clarity.

form intermediate **2**. This then cyclizes to form the oxo-anion intermediate **3**, which detaches from UiO-66-40 and forms the corresponding cyclic organic carbonate (intermediate **4**). Meanwhile, intermediate **1** also undergoes a nucleophilic addition reaction with the aromatic amine to form a ß-amino alcohol (intermediate **6**). The intermediates **4** and **6** react with each other in the presence of the free, basic alkylamine active sites to produce the corresponding oxazolidinone products with 1,2-diol as the byproduct.[19] It is noted that the intermediates **4** and **6** were separately synthesized to confirm their structures by ^{1}H NMR. Additionally, these intermediates **4** and **6** were reacted in order to demonstrate that they could in fact form the corresponding oxazolidinone (ESI, section S5†). This plausible mechanism for UiO-66-40 reveals a synergistic effect between two engineered catalytically active sites for promoting the three-component reaction.

Recyclability is an important parameter for assessing the industrial relevance of a given heterogeneous catalyst. UiO-66-40 was applied to the model reaction, from which, upon completion of the first reaction, the catalyst was easily separated *via* centrifugation, washed with methanol three times, and reactivated by drying at 100 °C. The catalyst was then reused in five consecutive reactions following the same process. Interestingly, there was no loss in catalytic activity or performance even after the fifth reaction (ESI, Fig. S43†). Furthermore, the structure of UiO-66-40 remained intact throughout as evidenced by PXRD analysis (ESI, Fig. S44†).

Conclusions

In conclusion, for the first time, the successful engineering of a heterogeneous MOF catalyst to incorporate dual active sites is reported for CO$_2$ fixation in the synthesis of oxazolidinones

at high yields. Importantly, the active sites are proposed to work synergistically and are effective for a wide range of aromatic amine and epoxide substrates over multiple cycles. Ongoing work is focused on definitively understanding the nature of the defect sites within UiO-66-40 that promote the material's exceptional catalytic behaviour.

Conflicts of interest

There are no conflicts to declare.

Acknowledgements

Notes and references

1 C. Hepburn, E. Adlen, J. Beddington, E. A. Carter, S. Fuss, N. Mac Dowell, J. C. Minx, P. Smith and C. K. Williams, The Technological and Economic Prospects for CO$_2$ Utilization and Removal, *Nature*, 2019, **575**, 87–97.

2 M. Cokoja, C. Bruckmeier, B. Rieger, W. A. Herrmann and F. E. Kuhn, Transformation of Carbon Dioxide with Homogeneous Transition–Metal Catalysts: A Molecular Solution to a Global Challenge?, *Angew. Chem., Int. Ed.*, 2011, **50**, 8510–8537; I. Omae, Recent Developments in Carbon Dioxide Utilization for the Production of Organic Chemicals, *Coord. Chem. Rev.*, 2012, **256**, 1384–1405.

3   J. A. Rodriguez, P. Liu, D. J. Stacchiola, S. D. Senanayake, M. G. White and J. G. Chen, Hydrogenation of CO_2 to Methanol: Importance of Metal–Oxide and Metal–Carbide Interfaces in the Activation of CO_2, *ACS Catal.*, 2015, **5**, 6696–6706; Q. Liu, L. Wu, R. Jackstell and M. Beller, Using Carbon Dioxide as a Building Block in Organic Synthesis, *Nat. Commun.*, 2015, **6**, 5933–5948; S. Dabral and T. Schaub, The Use of Carbon Dioxide (CO_2) as a Building Block in Organic Synthesis from an Industrial Perspective, *Adv. Synth. Catal.*, 2019, **361**, 223–246.

4   J. B. Locke, G. E. Zurenko, K. J. Shaw and K. Bartizal, Tedizolid: A Novel Oxazolidinone for Gram-Positive Infections, *Clin. Infect. Dis.*, 2014, **58**, S1–S3; M. A. Hedaya, V. Thomas, M. E. Abdel-Hamid, E. O. Kehinde and A. O. Phillips, A Validated UPLC–MS/MS Method for the Analysis of Linezolid and a Novel Oxazolidinone Derivative (PH027) in Plasma and its Application to Tissue Distribution Study in Rabbits, *J. Chromatogr. B: Anal. Technol. Biomed. Life Sci.*, 2017, **1040**, 89–96; M. R. Barbachyn and C. W. Ford, Oxazolidinone Structure–Activity Relationships Leading to Linezolid, *Angew. Chem., Int. Ed.*, 2003, **42**, 2010–2023.

5   C. S. Park, M. S. Kim, T. B. Sim, D. K. Pyun, C. H. Lee, D. Choi, W. K. Lee, J.-W. Chang and H.-J. Ha, Novel Stereoselective Synthesis of Functionalized Oxazolidinones from Chiral Aziridines, *J. Org. Chem.*, 2003, **68**, 43–49; J. A. Castro-Osma, A. Earlam, A. Lara-Sanchez, A. Otero and M. North, Synthesis of Oxazolidinones from Epoxides and Isocyanates Catalysed by Aluminium Heteroscorpionate Complexes, *ChemCatChem*, 2016, **8**, 2100–2108.

6   U. R. Seo and Y. K. Chung, Potassium phosphate-catalyzed one-pot synthesis of 3-aryl-2-oxazolidinones from epoxides, amines, and atmospheric carbon dioxide, *Green Chem.*, 2017, **19**, 803–808; S. Arshadi, E. Vessally, M. Sobati, A. Hosseinian and A. Bekhradnia, Chemical Fixation of CO_2 to N-propargylamines: A Straightforward Route to 2-Oxazolidinones, *J. CO_2 Util.*, 2017, **19**, 120–129; S. Arshadi, E. Vessally, A. Hosseinian, S. Soleimani-amiri and L. Edjlali, Three-Component Coupling of CO_2, Propargyl Alcohols, and Amines: An Environmentally Benign Access to Cyclic and Acyclic Carbamates (A Review), *J. CO_2 Util.*, 2017, **21**, 108–118.

7   H. Furukawa, K. E. Cordova, M. O'Keeffe and O. M. Yaghi, The Chemistry and Applications of Metal-Organic Frameworks, *Science*, 2013, **341**, 1230444; C. S. Diercks, Y. Liu, K. E. Cordova and O. M. Yaghi, The Role of Reticular Chemistry in the Design of CO_2 Reduction Catalysts, *Nat. Mater.*, 2018, **17**, 301–307; C. A. Trickett, A. Helal, B. A. Al-Maythalony, Z. H. Yamani, K. E. Cordova and O. M. Yaghi, The Chemistry of Metal–Organic Frameworks for CO_2 Capture, Regeneration and Conversion, *Nat. Rev. Mater.*, 2017, **2**, 17045.

8   L. Liu, Z. Chen, J. Wang, D. Zhang, Y. Zhu, S. Ling, K.-W. Huang, Y. Belmabkhout, K. Adil, Y. Zhang, B. Slater, M. Eddaoudi and Y. Han, Imaging Defects and their Evolution in a Metal–Organic Framework at Sub-Unit-Cell Resolution, *Nat. Chem.*, 2019, **11**, 622–628; S. Dissegna, K. Epp, W. R. Heinz, G. Kieslich and R. A. Fischer, Defective Metal–Organic Frameworks, *Adv. Mater.*, 2018, **30**, 1704501; M. R. De Stefano, T. Islamoglu, S. J. Garibay, J. T. Hupp and O. K. Farha, Room-Temperature Synthesis of UiO-66 and Thermal Modulation of Densities of Defect Sites, *Chem. Mater.*, 2017, **29**, 1357–1361; R. Wei, C. A. Gaggioli, G. Li, T. Islamoglu, Z. Zhang, P. Yu, O. K. Farha, C. J. Cramer, L. Gagliardi, D. Yang and B. C. Gates, Tuning the Properties of Zr_6O_8 Nodes in the Metal Organic Framework UiO-66 by Selection of Node-Bound Ligands and Linkers, *Chem. Mater.*, 2019, **31**, 1655–1663; G. C. Shearer, S. Chavan, S. Bordiga, S. Svelle, U. Olsbye and K. P. Lillerud, Defect Engineering: Tuning the Porosity and Composition of the Metal–Organic Framework UiO-66 via Modulated Synthesis, *Chem. Mater.*, 2016, **28**, 3749–3761.

9   G. Cai and H.-L. Jiang, A Modulator–Induced Defect–Formation Strategy to Hierarchically Porous Metal–Organic Frameworks with High Stability, *Angew. Chem., Int. Ed.*, 2017, **56**, 563–567; Y. Liu, R. C. Klet, J. T. Hupp and O. Farha, Probing the Correlations between the Defects in Metal–Organic Frameworks and their Catalytic Activity by an Epoxide Ring-Opening Reaction, *Chem. Commun.*, 2016, **52**, 7806–7809; F. G. Cirujano, A. Corma and F. X. L. Xamena, Conversion of Levulinic Acid into Chemicals: Synthesis of Biomass Derived Levulinate Esters over Zr-Containing MOFs, *Chem. Eng. Sci.*, 2015, **124**, 52–60; S. Dissegna, R. Hardian, K. Epp, G. Kieslich, M.-V. Coulet, P. Llewellyn and R. A. Fischer, Using Water Adsorption Measurements to Access the Chemistry of Defects in the Metal–Organic Framework UiO-66, *CrystEngComm*, 2017, **19**, 4137–4141; W. Zhang, M. Kauer, O. Halbherr, K. Epp, P. Guo, M. I. Gonzalez, D. J. Xiao, C. Wiktor, F. X. L. Xamena, C. Woll, Y. Wang, M. Muhler and R. Fischer, A. Ruthenium Metal–Organic Frameworks with Different Defect Types: Influence on Porosity, Sorption, and Catalytic Properties, *Chem. – Eur. J.*, 2016, **22**, 14297–14307; K. Leus, M. Vandichel, Y.-Y. Liu, I. Muylaert, J. Musschoot, S. Pyl, H. Vrielinck, F. Callens, G. B. Marin, C. Detavernier, P. V. Wiper, Y. Z. Khimyak, M. Waroquier, V. Van Speybroeck and P. Van Der Voort, The Coordinatively Saturated Vanadium MIL-47 as a Low Leaching Heterogeneous Catalyst in the Oxidation of Cyclohexene, *J. Catal.*, 2012, **285**, 196–207.

10 M. Vandichel, J. Hajek, F. Vermoortele, M. Waroquier, D. E. De Vos and V. Van Speybroeck, Active Site Engineering in UiO-66 Type Metal–Organic Frameworks by Intentional Creation of Defects: A Theoretical Rationalization, *CrystEngComm*, 2015, **17**, 395–406; T. H. Park, A. J. Hickman, K. Koh, S. Martin, A. G. Wong-Foy, M. S. Sanford and A. J. Matzger, Highly Dispersed Palladium(II) in a Defective Metal–Organic Framework: Application to C–H Activation and Functionalization, *J. Am. Chem. Soc.*, 2011, **133**, 20138–20141; S. Marx, W. Kleist and A. Baiker, Synthesis, Structural Properties, and Catalytic

Behavior of Cu-BTC and Mixed-Linker Cu-BTC-PyDC in the Oxidation of Benzene Derivatives, *J. Catal.*, 2011, **281**, 76–87.

11 H. Xu, X.-F. Liu, C.-S. Cao, B. Zhao, P. Cheng and L.-N. He, A Porous Metal–Organic Framework Assembled by [Cu30] Nanocages: Serving as Recyclable Catalysts for CO_2 Fixation with Aziridines, *Adv. Sci.*, 2016, **3**, 1600048; C.-S. Cao, Y. Shi, H. Xu and B. Zhao, A Multifunctional MOF as a Recyclable Catalyst for the Fixation of CO_2 with Aziridines or Epoxides and as a Luminescent Probe of Cr(vi), *Dalton Trans.*, 2018, **47**, 4545–4553.

12 J. H. Cavka, S. Jakobsen, U. Olsbye, N. Guillou, C. Lamberti, S. Bordiga and K. P. Lillerud, A New Zirconium Inorganic Building Brick Forming Metal Organic Frameworks with Exceptional Stability, *J. Am. Chem. Soc.*, 2008, **130**, 13850–13851.

13 F. Vermoortele, B. Bueken, G. Le Bars, B. V. de Voorde, M. Vandichel, K. Houthoofd, A. Vimont, M. Daturi, M. Waroquier, V. Van Speybroeck, C. Kirschhock and D. E. De Vos, Synthesis Modulation as a Tool to Increase the Catalytic Activity of Metal–Organic Frameworks: The Unique Case of UiO-66(Zr), *J. Am. Chem. Soc.*, 2013, **135**, 11465–11468; H. Wu, T. Yildirim and W. Zhou, Exceptional Mechanical Stability of Highly Porous Zirconium Metal–Organic Framework UiO-66 and Its Important Implications, *J. Phys. Chem. Lett.*, 2013, **4**, 925–930; Y. Bai, Y. Dou, L.-H. Xie, W. Rutledge, J.-R. Li and H.-C. Zhou, Zr-Based Metal–Organic Frameworks: Design, Synthesis, Structure, and Applications, *Chem. Soc. Rev.*, 2016, **45**, 2327–2367.

14 H. Wu, Y. S. Chua, V. Krungleviciute, M. Tyagi, P. Chen, T. Yildirim and W. Zhou, Unusual and Highly Tunable Missing-Linker Defects in Zirconium Metal–Organic Framework UiO-66 and Their Important Effects on Gas Adsorption, *J. Am. Chem. Soc.*, 2013, **135**, 10525–10532;

C. A. Trickett, K. J. Gagnon, S. Lee, F. Gandara, H.-B. Burgi and O. M. Yaghi, Definitive Molecular Level Characterization of Defects in UiO–66 Crystals, *Angew. Chem., Int. Ed.*, 2015, **54**, 11162–11167.

15 K. M. Choi, H. J. Jeon, J. K. Kang and O. M. Yaghi, Heterogeneity within Order in Crystals of a Porous Metal–Organic Framework, *J. Am. Chem. Soc.*, 2011, **133**, 11920–11923.

16 G. S. Mohammad-Pour, K. O. Hatfield, D. C. Fairchild, K. Hernandez-Burgos, J. Rodriguez-Lopez and F. J. Uribe-Romo, A Solid-Solution Approach for Redox Active Metal–Organic Frameworks with Tunable Redox Conductivity, *J. Am. Chem. Soc.*, 2019, **141**, 19978–19982; A. Helal, Z. H. Yamani, K. E. Cordova and O. M. Yaghi, Multivariate Metal-Organic Frameworks, *Natl. Sci. Rev.*, 2017, **4**, 296–298; Y.-B. Zhang, H. Furukawa, N. Ko, W. Nie, H. J. Park, S. Okajima, K. E. Cordova, H. Deng, J. Kim and O. M. Yaghi, Introduction of Functionality, Selection of Topology, and Enhancement of Gas Adsorption in Multivariate Metal–Organic Framework-177, *J. Am. Chem. Soc.*, 2015, **137**, 2641–2650.

17 K. Sumida, D. L. Rogow, J. A. Mason, T. M. McDonald, E. D. Bloch, Z. R. Herm, T.-H. Bae and J. R. Long, Carbon Dioxide Capture in Metal–Organic Frameworks, *Chem. Rev.*, 2012, **112**, 724–781.

18 C. Atzori, G. C. Shearer, L. Maschio, B. Civalleri, F. Bonino, C. Lamberti, S. Svelle, K. P. Lillerud and S. Bordiga, Effect of Benzoic Acid as a Modulator in the Structure of UiO-66: An Experimental and Computational Study, *J. Phys. Chem. C*, 2017, **121**, 9312–9324.

19 U. R. Seo and Y. K. Chung, Potassium Phosphate-Catalyzed One-Pot Synthesis of 3-Aryl-2-Oxazolidinones from Epoxides, Amines, and Atmospheric Carbon Dioxide, *Green Chem.*, 2017, **19**, 803–808.